

Object orientation in two dimensional grasp with friction towards minimization of gripping power

Satoshi Ito · Shouta Takeuchi · Minoru Sasaki

Received: 12 March 2009 / Accepted: 20 August 2009 / Published online: 26 September 2009
© Springer-Verlag 2009

Abstract This article reports an analysis of two dimensional grasp where a convex rigid object is grasped by two contact points with friction. The purpose is to find the object orientation that minimizes the norm of the contact force vector, each element of which is composed from the normal force and friction force at each contact point. The formulation of this problem requires some equality or inequality conditions. In the analysis, the solution of the equality conditions is parameterized at first. Based on the fact that the norm of the contact force vector becomes monotonic increasing function of this parameter, the minimal parameter values are calculated by means of the piecewise analysis. Using the relation between the friction coefficient and the apex angle of the friction cone effectively, the following result is obtained: the norm of the contact force, i.e. gripping power becomes locally minimal at the object orientation where the intersection point of the upper sides of two friction cones is located in opposite direction of the gravity from the center of mass of the grasped object.

Keywords Grasping · Minimization · Gripping power · Friction · Object orientation

1 Introduction

Grasping an object is an essential function for humans. Because the grasp is a task with redundancy, there are many possibilities for performing it. For example, there are many combinations of the contact points, i.e., places that the fingers touch to grasp the object. When these contact points are

assigned, the amount or direction of the contact forces is not determined uniquely. The direction of the grasped object is sometimes selected arbitrarily.

Such many possibilities originate from the ill-posedness of the grasping problem. To grasp an object firmly, some conditions or constraints are required (Nguyen 1988; Bicchi 1995). However, many degrees of freedom of the grasping mechanisms like fingers allow multiple solutions even under these constraints.

Methods for tackling to the grasping problem including the ill-posedness are widely ranging, by use of neuronal (Oztop and Arbib 2002; Shim et al. 2003; Frey et al. 2005), behavioral (Zatsiorsky and Latash 2008), computational (including analytical) (Shimoga 1996; Borst et al. 1999; Miller and Allen 2000; Miller et al. 2003; Lopez-Damian et al. 2005; Ciocarlie et al. 2007; Huebner et al. 2008; Roa and Suárez 2009), or constructive (robotic) (Arimoto et al. 2001; Dollar and Howe 2005; Berenson and Srinivasa 2008) approaches. Among them, this article adopts an analytical method: to elucidate the physical meaning of the grasping task theoretically not only provides reasonable evidences for understanding human strategies in the grasp but also deduces beneficial knowledge on medical therapy for hand motions, prosthetic hand control or robotic hand manipulations in the factories. The framework of optimization is a standard analytical method for ill-posed problems. Many studies on grasp have been reported as an optimization problem with various kinds of an evaluation function or an optimizing factor. Regarding the evaluation function, the norm of the contact force vector is often selected. Some studies minimize the component that compensates for the gravitational force of the object (Markenscoff and Papadimitriou 1989) or the component required to balance the normalized external force (Mirtich and Canny 1994; Mangialardi et al. 1996). Regarding to an evaluation of the power grasp, Nakamura

S. Ito (✉) · S. Takeuchi · M. Sasaki
Department of Human and Information Systems, Faculty
of Engineering, Gifu University, Yanagido 1-1, Gifu 501-1193, Japan
e-mail: satoshi@gifu-u.ac.jp

et al. focused on the external force just before the object starts moving (Zhang et al. 1994) and created an algorithm for calculating this force (Nakamura and Kurushima 1997). A power output of the grasping mechanisms was proposed as another evaluation function (Yong et al. 1998; Watanabe and Yoshikawa 2003). Regarding the optimizing factors, on the other hand, the placement of the contact points has been generally treated (Markenscoff and Papadimitriou 1989; Mirtich and Canny 1994; Mangialardi et al. 1996), though some articles have considered the posture of the grasping mechanisms (Yong et al. 1998; Watanabe and Yoshikawa 2003) or the range of the contact point placement while keeping the force balance in three dimensional space (Omata 1993). A method for solving the optimization problems were another issue in grasping. They were sometimes translated to linear (Cheng and Orin 1990; Liu 1999) or quadratic programming (Ding et al. 2001) by approximating friction cones using polyhedral cones. An artificial neural network (Xia et al. 2004; Al-Gallaf 2006) is another powerful method, and fuzzy logic was utilized for aiming at real-time applications (Dubey et al. 1999).

Among some optimizing factors such as the placement of the contact points and the magnitude of the internal forces or joint torques of the grasping mechanisms, the posture of the grasped object is considered in this article. The posture here means the spacial relation to the world coordinate frame—in other words, to the direction of gravity. This problem originates from our following observation: although some persons can grasp a large ball only with one hand, as shown in Fig. 1, one of authors cannot do. Of course, the smallness of his hand is a fatal reason: when a hand is large, the contact points on the ball surface can be selected so that the distance between them become large, which easily satisfies contact point conditions: friction cones at the contact points on the ball include the other contact points (see Sect. 2.3.1). Then, large internal forces can be applied without the contact points slipping, resulting in that the forces com-



Fig. 1 One hand grasp of a large ball

pensating the gravity can be generated using the frictions. However, there is a case where a person cannot grasp the ball because he/she cannot generate enough large internal forces. So, the following questions naturally arise: which posture is the most possible to achieve with a less gripping power?—if he/she cannot grasp an object at this posture, he/she cannot grasp it at any other postures. Thus, the aim of this article is to elucidate the posture that requires the least forces for grasping an object. The grasp with the less gripping power is preferable from the energetic point of view, as well as because it has less possibility of breaking a grasped object. However, such an issue was not sufficiently discussed in the previous studies mentioned above. In our previous studies (Ito et al. 2006), the friction was not considered. In this study, it is extended to the grasp with frictions, and the relation between an object orientation and the contact forces are discussed to grasp it by the least contact force. This issue is specific to the grasped object, in other words, independent of the grasping mechanisms such as fingers or grippers, although many studies treated the grasp including grasping mechanisms (Cole and Abbs 1987; Iberall and MacKenzie 1990; Yong et al. 1998; Watanabe and Yoshikawa 2003). Such object-specific matters probably include a universal fact commonly found in various kinds of the grasping mechanisms. In the next section, this topic is formulated as a minimization problem of the norm of the contact force vector. In Sect. 3, a method for solving this problem as well as the results are described, while their calculation processes are shown after in the appendices. These results are examined using some case studies in Sect. 4, and the article is concluded in Sect. 5.

2 Grasp with frictions

2.1 Assumptions

The following assumptions allow us to solve the problem here in an analytical, not numerical, manner.

- An object is grasped by the two contact points within the two dimensional (2D) space.
- The object is convex and rigid.
- The shape of the object is smooth at the contact points.
- The contacts on the object are the point contacts with the friction.

As an evaluation of the object orientation, the magnitude of the contact forces is selected: larger contact forces than necessary might damage the object. Above all, grasping with less contact forces allowed us to efficiently maintain the grasped posture with small gripping power.

Fig. 2 Coordinate frames

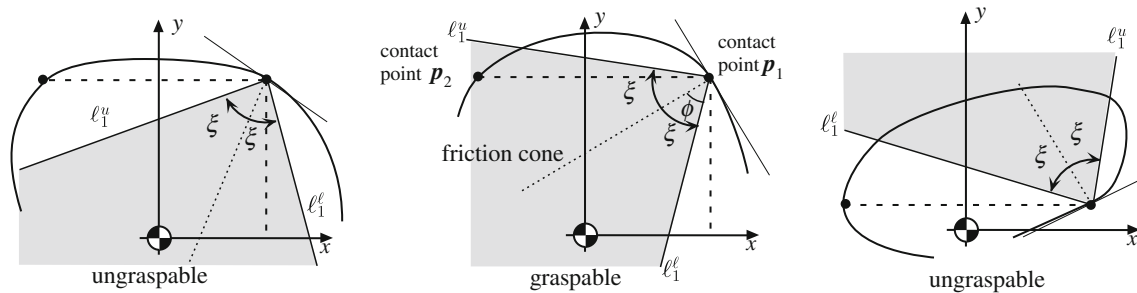
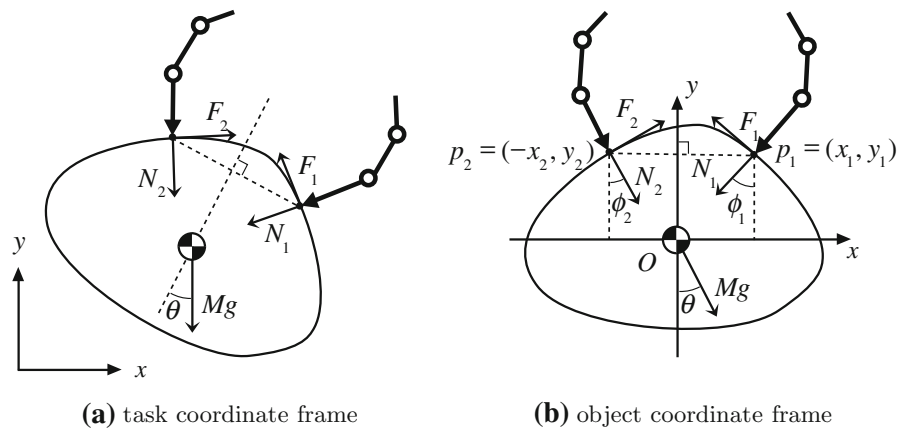


Fig. 3 Cases where the object can be grasped or not be grasped

2.2 Coordinate frame for analysis

The object grasped by two contact points in the 2D space is illustrated in Fig. 2a. The object posture with respect to the gravitational direction is represented by the angle θ . The problem is formulated in the following way: what value should be chosen for θ in order to grasp this object with less contact forces.

This problem is easily described in the object coordinate frame in which the origin is set to the center of mass (CoM) of the object and the y axis is defined to be orthogonal to the line connecting two contact points as shown in Fig. 2b. In this object coordinate frame, the object orientation is represented as the relative angle of the gravity vector from the negative direction of the y axis.

In the object coordinate frame, the coordinate of the two contact points are denoted by $p_1 = (x_1, y)^T$ and $p_2 = (-x_2, y)^T (\neq p_1)$, and the normal direction at these contact points are, ϕ_1 (CW) and ϕ_2 (CCW), from the negative direction of the y axis. Here, $x_1 > 0, x_2 > 0, y > 0$, and $0 < \phi_1 \leq \pi/2, 0 < \phi_2 \leq \pi/2$. The contact forces are orthogonally decomposed to the normal force N_i and the friction F_i ($i = 1, 2$) at each contact point.

2.3 Formulation

2.3.1 Contact point conditions

If both friction cones contain the other contact point, then the object can be grasped by these two contact points (Nguyen 1988). This condition can be described with inequalities. As shown in Fig. 3, the apex angle of the friction cone is set to 2ξ . The upper and lower side of the friction cone is denoted by ℓ^u and ℓ^ℓ , respectively. The object is graspable if and only if the relative angle of ℓ^u is greater than $\pi/2$ as well as the relative angle of ℓ^ℓ is less than $\pi/2$, where the relative angle is measured from the negative direction of the y axis in the object coordinate frame. These conditions become

$$\phi_i - \xi_i < \frac{\pi}{2} < \phi_i + \xi_i \tag{1}$$

The above conditions can be rewritten with the friction coefficient μ_i at each contact point. The following relation holds between the apex angle and the friction coefficient.

$$\tan \xi_i = \mu_i \tag{2}$$

Thus, subtract ϕ_i from (1), apply tangent operation for this result, and use the relation (2). Then, the following inequality is obtained:

$$s_i \mu_i + c_i > 0, s_i \mu_i - c_i > 0 \tag{3}$$

Here, $s_i = \sin \phi_i, c_i = \cos \phi_i$.

2.3.2 Force balance conditions

In the 2D grasp, not only the force in the x and y direction but also the moment within the plane including both coordinate axes must be balanced. This balancing condition is described using matrix as

$$L\mathbf{F} = \mathbf{M} \tag{4}$$

where the contact force vector \mathbf{F} and the gravity vector \mathbf{M} is defined as follows:

$$\mathbf{F} = [N_1 \ F_1 \ N_2 \ F_2]^T \tag{5}$$

$$\mathbf{M} = [-Mgs \ Mgc \ 0]^T \tag{6}$$

Here, M is mass of the object, g is the gravitational acceleration, $s = \sin \theta$ and $c = \cos \theta$. The matrix, L , is called grasp matrix, and described as

$$L = \begin{bmatrix} -s_1 & -c_1 & s_2 & c_2 \\ -c_1 & s_1 & -c_2 & s_2 \\ L_{31} & L_{32} & L_{33} & L_{34} \end{bmatrix} \tag{7}$$

$$L_{31} = -c_1 x_1 + s_1 y, \ L_{32} = +s_1 x_1 + c_1 y$$

$$L_{33} = +c_2 x_2 - s_2 y, \ L_{34} = -s_2 x_2 - c_2 y$$

2.3.3 Grasping conditions

Grasping the object from the above with frictions is the focus of this study. Other cases, as illustrated with a shaded range in Fig. 4, should be excluded, because the object can be kept on the grasping mechanism just by being overridden on it, i.e., without actively grasping the object. This is why the range of the gravitational direction θ is restricted as

$$\theta_{\min} < \theta < \theta_{\max} \tag{8}$$

where

$$\theta_{\min} = -\pi + \arctan 2(x_2, y) \tag{9}$$

$$\theta_{\max} = \pi - \arctan 2(x_1, y) \tag{10}$$

This range is illustrated by the arrowed line in Fig. 4. Here, $\arctan 2(Y, X)$ returns $\tan^{-1}(Y/X)$ in the range $[-\pi, \pi]$.

2.3.4 Contact force conditions

The normal force is repulsive, i.e., works so as to push the object. Thus,

$$(i) \ N_1 > 0 \tag{11}$$

$$(ii) \ N_2 > 0 \tag{12}$$

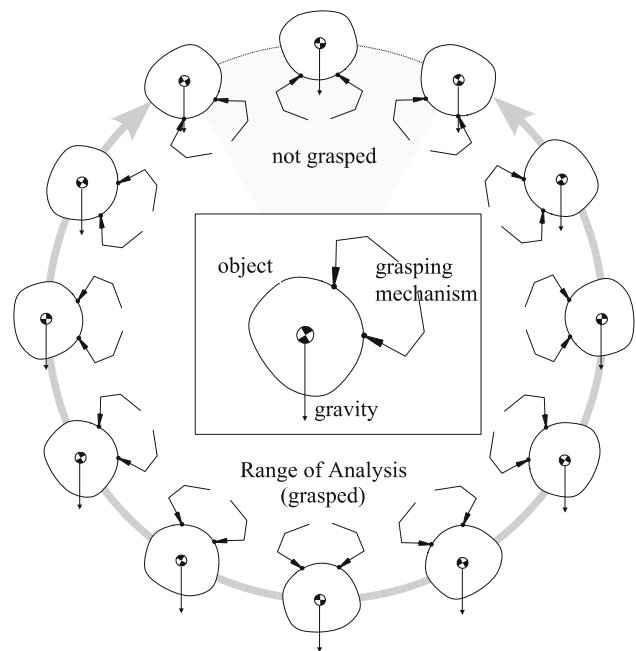


Fig. 4 Range of analysis

must hold. In addition, the vector of the contact force must be included within the friction cone. In other words, to keep the contact without slipping, the tangential force never exceeds the maximal static friction force. It holds if $|F_i| < \mu_i N_i$. This condition can be decomposed to the following four inequalities.

$$(iii) \ \mu_1 N_1 - F_1 > 0 \tag{13}$$

$$(iv) \ \mu_2 N_2 - F_2 > 0 \tag{14}$$

$$(v) \ \mu_1 N_1 + F_1 > 0 \tag{15}$$

$$(vi) \ \mu_2 N_2 + F_2 > 0 \tag{16}$$

2.3.5 Problem description

Now, the problem can be mathematically described as follows:

Definition 1 Under the contact point condition (3), find θ , within the range (8), that minimizes the norm of the contact force vector \mathbf{F} satisfying the force balance condition (4) as well as the contact force conditions (11)–(16).

3 Analysis

3.1 Methods

The problem defined in the above section is one class of the nonlinear optimization problems. Here, the following procedure is taken to analytically solve it.

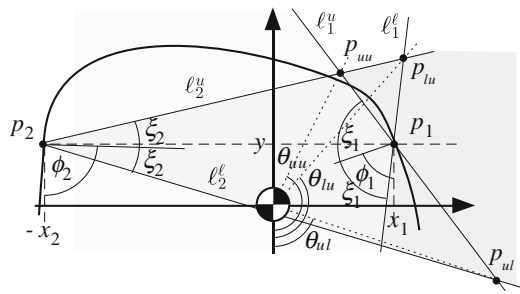


Fig. 5 Relative direction of friction-cones' intersection point

Step 1 Describe the solution of the force balance condition given by equality (4) as a family of one parameter α .

From the physical point of view, α denotes an amount proportional to the magnitude of the internal force. As we can imagine, the norm of contact force vector F becomes a monotonic increasing function of the parameter α , regardless of the norm selection such as 1- or 2-norm. It indicates that a smaller α gives a better solution. Therefore, the minimization of the norm of F is replaced by that of the parameter α . However, the parameter α must be selected so that all the inequality conditions should hold. Thus, α is minimized by the following steps:

Step 2 Calculate the lower limit of the parameter α for respective inequality (11)–(16).

Here, let $\alpha_k(\theta)$ ($k = 1, \dots, 6$) to be the minimal α that satisfies only one of the inequalities (i)–(vi).

Step 3 Construct the lower limit of the feasible solution based on the result of the Step 2, and denote it to $\alpha_{\min}(\theta)$.

Any α greater than or equal to α_{\min} in each θ satisfy all the inequality conditions (i)–(vi). Therefore, $\alpha_{\min}(\theta)$ is constructed by selecting the maximal $\alpha_k(\theta)$ in each θ . This process is equivalent to the comparison of the $\alpha_k(\theta)$ in the piecewise range of θ .

Step 4 Analyze the minimal point of $\alpha_{\min}(\theta)$ and its physical interpretation.

The minimal solution of this problem is given as the minimum point of $\alpha_{\min}(\theta)$. The physical meanings of the minimal solution is analyzed to clarify the orientation of the grasped object in the task coordinate frame.

3.2 Results

Details of calculations are described in the appendices. Only the results are shown here. The results depend on the intersection point of the friction cones. Thus, following notation is defined here as shown in Fig. 5: Let l_1^u and l_1^l to

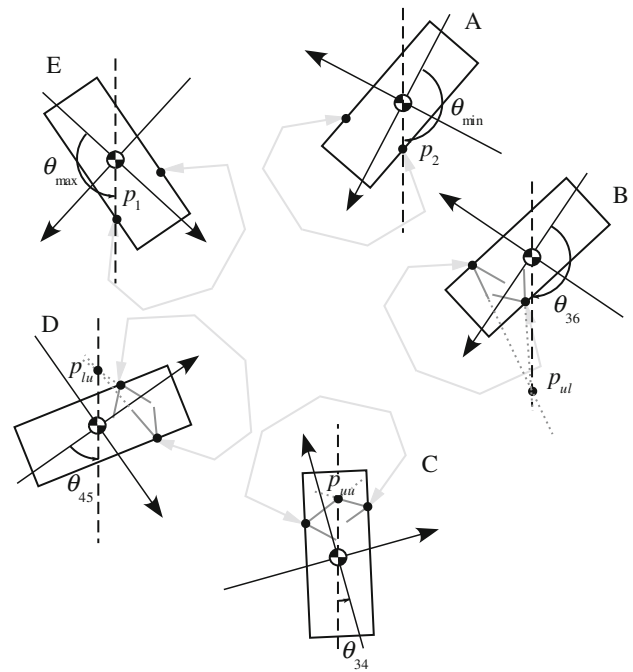


Fig. 6 Object orientations that gives a local minimal point

be the upper and lower side of the friction cone at the contact point p_1 , respectively. So do l_2^u and l_2^l for p_2 . Then define $p_{uu}(X_{uu}, Y_{uu})$, $p_{ul}(X_{ul}, Y_{ul})$, $p_{lu}(X_{lu}, Y_{lu})$ as an intersection point of l_1^u and l_2^u , l_1^u and l_2^l , l_1^l and l_2^u , respectively.

Our results here can be summarized as the following theorem.

Theorem 1 When a convex rigid object is grasped by two contact points with friction in 2D space, minimize the norm of the contact force vector by the object orientation. Then, there are five candidates for the local minimal point, as shown in Fig. 6. In each posture, the CoM of the object is

- A. Above the contact point p_2 .
- B. Above or below the intersection point of friction cone's sides p_{ul} .
- C. Below the intersection point of friction cone's sides p_{uu} .
- D. Above or below the intersection point of friction cone's sides p_{lu} .
- E. Above the contact point p_1 .

The local minimum point is selected from these candidates based on the spatial relation among the friction cones and the CoM of the object as follows:

The local minimum points are

- (a) A, C, E, if both friction cones include the CoM of the object.

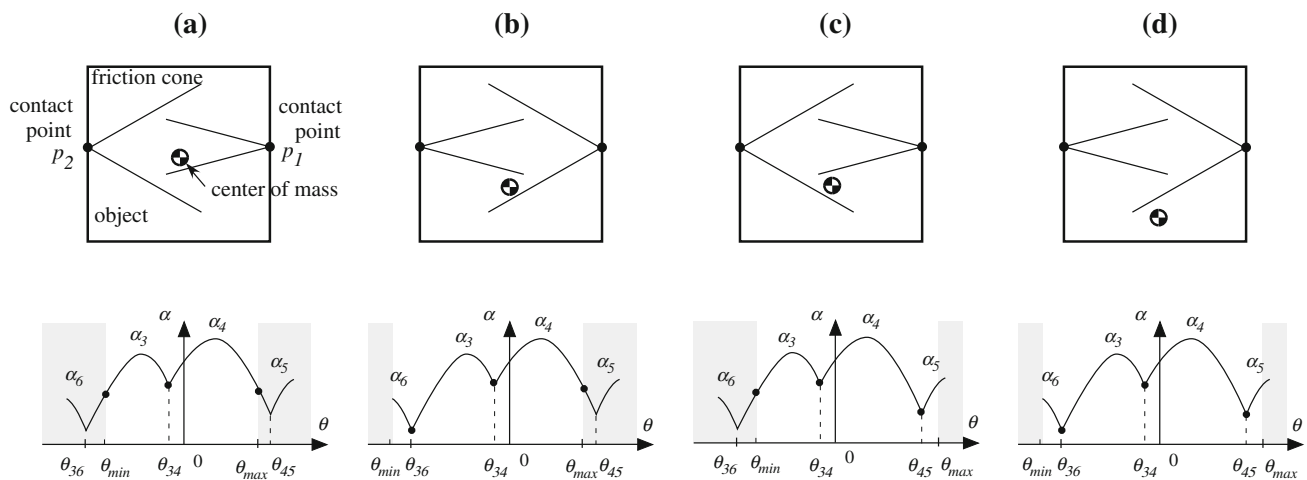


Fig. 7 Classification of minimum point with α_{\min}

- (b) *B, C, E, if the friction cone of the contact point p_1 include the CoM of the object, but the other does not.*
 (c) *A, C, D, if the friction cone of the contact point p_2 include the CoM of the object, but the other does not.*
 (d) *B, C, D, if neither friction cones include the CoM of the object.*

Each case is illustrated in the upper side of Fig. 7. The graphs in the lower side shows the typical shape of the function $\alpha_{\min}(\theta)$ representing the relations of the object orientation to the minimally required internal force. The θ_{\min} , θ_{36} , θ_{34} , θ_{45} , and θ_{\max} respectively correspond to the object orientation in case A, B, C, D, and E, as shown in Fig. 6. Refer to appendix for detail.

In all the cases except case C, the object is grasped from the side: our original interest is the case when the object is grasped from the above. Such a meaningful solution is only given as the case C. This result is consistent to our numerical analysis on the special case, grasp of the circular object (Ito et al. 2007).

4 Case studies

Four sample cases as shown in Fig. 8 are analyzed. In case (a), the simplest circular object is considered to intuitively understand the validity of our analysis. In case (b), a rectangular object is pinched up with neighboring edges. A rectangular object where one friction cone does not include its CoM is addressed in case (c), while one whose CoM is not included in neither friction cones in case (d). Parameters in the case studies are arranged in Table 1. In each case, $Mg = 1$.

All the α_k ($k = 1, \dots, 6$) as well as the norm of the contact force vector F are calculated within the range given by (8).

The results of the graphs are depicted in Fig. 9. The graph in the left side shows α_k changing with θ . The feasible solution α is in the area that is greater than all α_k 's ($k = 1, \dots, 6$). The minimal norm for these feasible solutions are drawn at the graph in the right side. Both 1- and 2-norm are calculated for each case. The candidates of the minimal point that is calculated from the parameters are summarized in Table 2.

As shown in Fig. 7, θ_{\min} , θ_{34} , and θ_{\max} become the local minimal point in the cases (a) and (b), while θ_{36} , θ_{34} , and θ_{\max} does in the case (c), regardless of the norm selection. When the 1-norm is selected, the smoothness is often disturbed at the point where the sign of F_1 or F_2 alters. In the case (d), though θ_{34} and θ_{45} are minimal points as shown in Fig. 7d, θ_{36} is not strictly speaking. However, it is valid for the candidate of the minimal point. In all cases, the minimal point of our interest is given as θ_{34} .

5 Discussion and concluding remarks

In this article, a 2D grasp is analyzed. An object is convex, rigid, and is grasped with two given contact points with friction. The object grasp requires some equality conditions, i.e., the force balance conditions, as well as some inequality conditions, i.e., the contact point conditions and the contact force conditions consisting of the normal force conditions and friction conditions. Among many feasible grasp, the object orientation that minimizes the norm of the contact force vector is mathematically analyzed. Here, contact force vector is the one whose element is composed from the normal and friction force at each contact point.

In the analysis, the solution of the equality conditions are parameterized at first. Then, the minimal parameter values are calculated by the piecewise analysis since the norm of

Fig. 8 Sample studies of the grasping

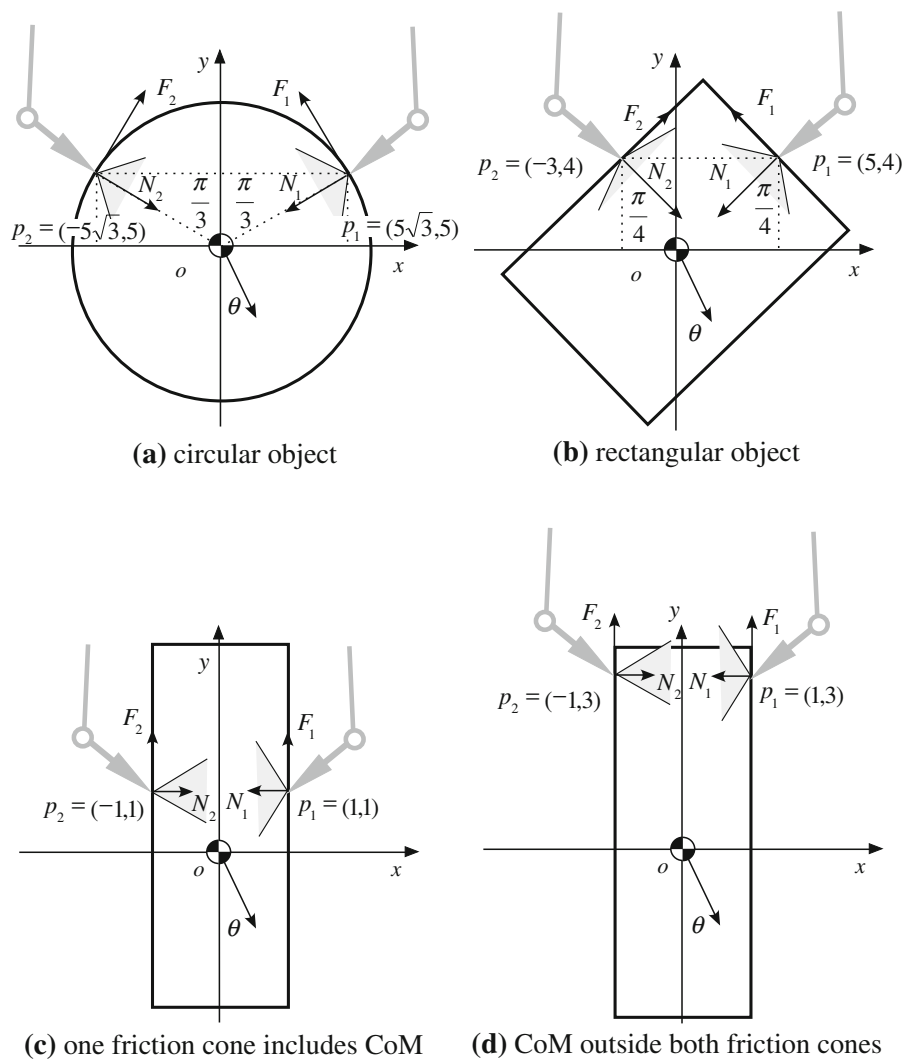


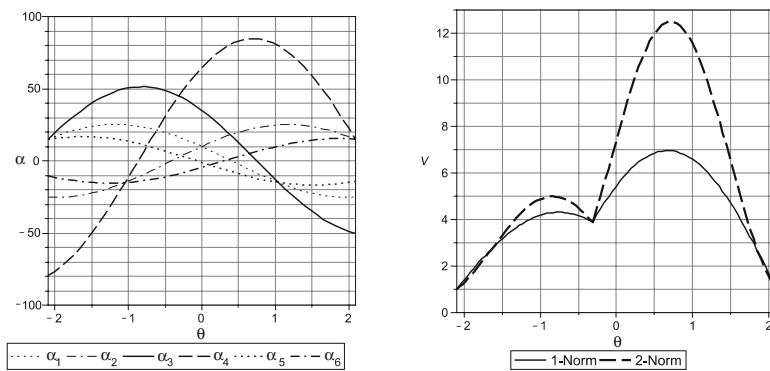
Table 1 Parameters in case studies

	p_1	p_2	ϕ_1	ϕ_2	μ_1	μ_2
(a)	$(5\sqrt{3}, 5)$	$(-5\sqrt{3}, 5)$	$\pi/3$	$\pi/3$	1.5	1.0
(b)	$(5, 4)$	$(-3, 4)$	$\pi/4$	$\pi/4$	1.5	2.5
(c)	$(1, 1)$	$(-1, 1)$	$\pi/2$	$\pi/2$	$\sqrt{3}$	$1/\sqrt{3}$
(d)	$(1, 3)$	$(-1, 3)$	$\pi/2$	$\pi/2$	$\sqrt{3}$	$1/\sqrt{3}$

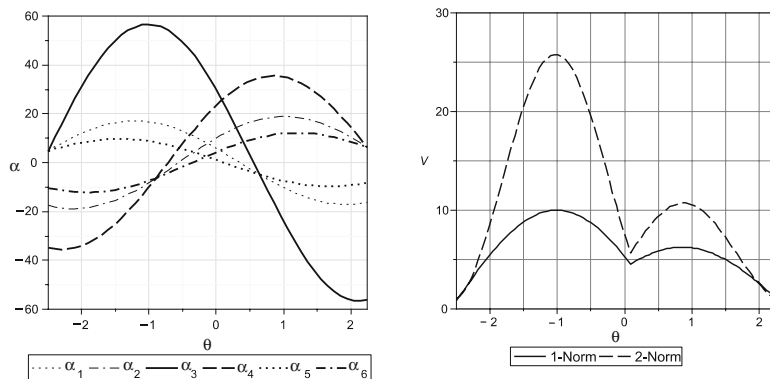
Table 2 Candidates of minimal point

	θ_{\min}	θ_{\max}	θ_{36}	θ_{34}	θ_{45}
(a)	-2.094	2.094	-2.491	-0.311	2.397
(b)	-2.498	2.498	-2.733	0.089	2.594
(c)	-2.356	2.356	-1.921	0.261	2.510
(d)	-2.820	2.820	-1.006	-0.129	2.742

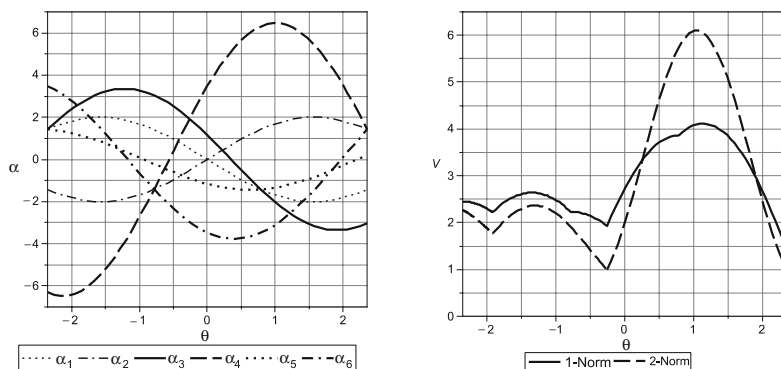
Fig. 9 Results of numerical calculations



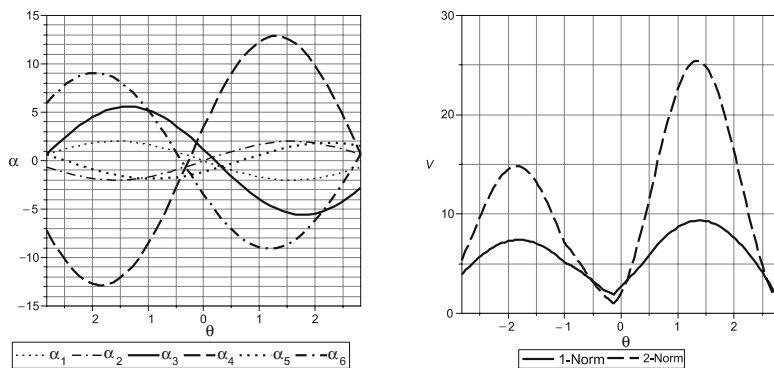
(a) circular object



(b) rectangular object



(c) the case (c) in Fig. 7



(d) the case (d) in Fig. 7

the contact force vector becomes monotonic increasing function of this parameter. Using the relation between the friction coefficient and the apex angle of the friction cone effectively, the following facts are clarified:

- There are five possible object orientations that minimize the magnitude of the contact forces. Two are the ones where the CoM of the object is located just above one of the contact points. The remaining three are the ones where the CoM and the intersection point of the sides of two friction cones align vertical on the gravity line.
- The spatial relation among the CoM of the object and friction cones determines which type of minimal point appears in the range where the object is grasped from above.
- The meaningful local minimal point where the object is grasped from above is the posture where the intersection point of the upper sides of each friction cone at two contact points is located in opposite direction of the gravity from the CoM of the object.

An analytical approach in this article elucidates one significant result; “an object is grasped with minimal gripping power when the intersection point of the friction cones sides and the CoM of the object aligns in the vertical direction”, which corresponds to the last one of the above three facts. This result may be applied to a hand rehabilitation training protocol for weak gripping-force patients, or an efficient robot’s grasping task planning. However, to understand a human grasping strategy, some verification experiments based on human measurements are needed. It is convenient for the discussion of its validness to reinterpret it as follows; “an object is grasped with minimal gripping power in the situation where two contact points are about to slip at the same time.” The meaningful minimal point of the norm of the contact force vector is θ_{34} , in which both contact points P_1 and P_2 are about to slip, because this point is determined as the intersection point of α_3 , the curve on which the contact point P_1 is about to slip, and α_4 , the curve for P_2 . Now let us consider the case where we reduce gripping power during the grasp with frictions. If one of the contact points comes near to slip, we will avoid it by adjusting the object orientation—so we will for another contact point; thus, final situation is the one where two contact points just start to slip simultaneously. This is the same as the above reinterpretation, implying that our result seems to be valid from our experiences. Of course, to ensure its rightness, the rigid verification including accurate measurement of, e.g., friction forces, is required.

In addition, we extend this analysis to the 3D grasp, and to the effective manipulation of the object requiring less contact forces as our future studies.

Appendices

A Parameterization of equality solution

The general solution of the equality (4) is given as

$$F = L^\dagger M + (I - L^\dagger L)\kappa \tag{17}$$

where L^\dagger is a pseudo-inverse matrix of L that can be calculated as $L^\dagger = L^T(LL^T)^{-1}$, and $\kappa \in R^4$ is an arbitrary vector. Let the first term of the right hand side be F_T . Then F_T is given from the definition as follows:

$$F_T = \frac{Mg}{2(x_1 + x_2)} \begin{bmatrix} (x_1 + x_2)s_1s + 2(ys - x_2c)c_1 \\ (x_1 + x_2)c_1s - 2(ys - x_2c)s_1 \\ -(x_1 + x_2)s_2s - 2(ys + x_1c)c_2 \\ -(x_1 + x_2)c_2s + 2(ys + x_1c)s_2 \end{bmatrix} \tag{18}$$

On the other hand, the second term of the right hand side is a vector that exists in $\text{Ker}L$, the kernel space of the matrix L . The dimension of the $\text{Ker}L$ is one since $\text{rank } L = 3$. Thus, the second term is written as follows:

$$(I - L^\dagger L)\kappa = \alpha F_N \tag{19}$$

$$F_N = \frac{Mg}{2(x_1 + x_2)} \begin{bmatrix} s_1 \\ c_1 \\ s_2 \\ c_2 \end{bmatrix} \tag{20}$$

Here, α is a scalar value that is proportional to the magnitude of the internal force exerted to the object, and F_N is a vector that satisfies the next two equations.

$$L F_N = \mathbf{0} \tag{21}$$

$$F_T^T F_N = 0 \tag{22}$$

From the definition of this section, the solution of the equality (4) is expressed, using F_T and F_N , as

$$F = F_T + \alpha F_N \tag{23}$$

B Lower limit calculation for each inequality

In this section, the calculations of the Step 2 in Sect. 3.1 are presented. The $\alpha_k(\theta)$ ($k = 1, \dots, 6$) defined in Sect. 3.1 is calculated in order. At first, $\alpha_1(\theta)$ is considered. From (23), N_1 is given as

$$N_1 = \frac{Mg}{2(x_1 + x_2)} ((x_1 + x_2)s_1s - 2(x_2c - ys)c_1 + \alpha s_1) \tag{24}$$

This equation leads to the lower limit of α that satisfies the inequality (i). So does it for $\alpha_2(\theta)$. Consequently, the following results are obtained:

$$\alpha > \alpha_k(\theta) \quad (k = 1, 2) \tag{25}$$

$$\alpha_1(\theta) = -(x_1 + x_2)s + 2(x_2c - ys) \cot \phi_1 \tag{26}$$

$$\alpha_2(\theta) = +(x_1 + x_2)s + 2(x_1c + ys) \cot \phi_2 \tag{27}$$

Next, $\alpha_3(\theta)$ is considered. From (23), F_1 is given as

$$F_1 = \frac{Mg}{2(x_1 + x_2)} ((x_1 + x_2)c_1s - 2(ys - x_2c)s_1 + \alpha c_1) \tag{28}$$

The equation (24) and (28) lead to the lower limit of α that satisfies the inequality (iii). So does it for $\alpha_4(\theta)$, $\alpha_5(\theta)$, and $\alpha_6(\theta)$. The results become

$$\alpha > \alpha_k(\theta) \quad (k = 3, \dots, 6) \tag{29}$$

$$\alpha_3(\theta) = -(x_1 + x_2)s + 2(x_2c - ys) \cdot \frac{c_1\mu_1 + s_1}{s_1\mu_1 - c_1} = -(x_1 + x_2)s - 2(x_2c - ys) \tan(\phi_1 + \xi_1) \tag{30}$$

$$\alpha_4(\theta) = +(x_1 + x_2)s + 2(x_1c + ys) \cdot \frac{c_2\mu_2 + s_2}{s_2\mu_2 - c_2} = +(x_1 + x_2)s - 2(x_1c + ys) \tan(\phi_2 + \xi_2) \tag{31}$$

$$\alpha_5(\theta) = -(x_1 + x_2)s + 2(x_2c - ys) \cdot \frac{c_1\mu_1 - s_1}{s_1\mu_1 + c_1} = -(x_1 + x_2)s - 2(x_2c - ys) \tan(\phi_1 - \xi_1) \tag{32}$$

$$\alpha_6(\theta) = +(x_1 + x_2)s + 2(x_1c + ys) \cdot \frac{c_2\mu_2 - s_2}{s_2\mu_2 + c_2} = +(x_1 + x_2)s - 2(x_1c + ys) \tan(\phi_2 - \xi_2) \tag{33}$$

In the above calculation, the next relation is used.

$$\frac{c_i\mu_i \pm s_i}{s_i\mu_i \mp c_i} = \frac{s_i \pm c_i\mu_i}{c_i \mp s_i\mu_i} = \frac{\frac{s_i}{c_i} \pm \mu_i}{1 \mp \frac{s_i}{c_i}\mu_i} = \frac{\tan \phi_i \pm \tan \xi_i}{1 \mp \tan \phi_i \tan \xi_i} = \tan(\phi_i \pm \xi_i) \tag{34}$$

Here, the Eq. 2 is applied to this calculation.

C Piecewise analysis for feasible solution

Based on some piecewise analyses, the magnitude relation among $\alpha_k(\theta)$ ($k = 1, \dots, 6$) is discussed. This process corresponds to the step 3 in Sect. 3.1. Firstly, the following relation holds.

Lemma 1 Let $\theta_1 = \arctan2(x_2, y) (> 0)$. $\alpha_5(\theta) < \alpha_1(\theta) < \alpha_3(\theta)$ holds in the range $\theta_{\min} < \theta < \theta_1$, while $\alpha_3(\theta) < \alpha_1(\theta) < \alpha_5(\theta)$ does in the range $\theta_1 < \theta < \theta_{\max}$.

Proof Calculating $\alpha_3 - \alpha_1$ (or $\alpha_5 - \alpha_1$), the following equation is obtained

$$2(x_2c - ys) \left(\frac{c_1\mu_1 \pm s_1}{s_1\mu_1 \mp c_1} - \frac{c_1}{s_1} \right) = \mp \frac{2}{s_1(s_1\mu_1 \mp c_1)} \sqrt{x_2^2 + y^2} \sin(\theta - \theta_1) \tag{35}$$

Here, $\sin(\theta - \theta_1) > 0$ in $\theta_1 < \theta < \theta_{\max}$ and $\sin(\theta - \theta_1) < 0$ in $\theta_{\min} < \theta < \theta_1$, because of $s_1 > 0$ and (3). Thus, the lemma is proved. \square

The next lemma also holds from the similar calculations.

Lemma 2 Let $\theta_2 = \arctan2(x_1, y) (> 0)$. $\alpha_4(\theta) < \alpha_2(\theta) < \alpha_6(\theta)$ holds in the range $\theta_{\min} < \theta < -\theta_2$, while $\alpha_6(\theta) < \alpha_2(\theta) < \alpha_4(\theta)$ holds in the range $-\theta_2 < \theta < \theta_{\max}$.

From the above two lemmas, the magnitude of α_i has only to be compared in the next combinations:

- α_3 versus α_6 in the range $\theta_{\min} < \theta < -\theta_2$.
- α_3 versus α_4 in the range $-\theta_2 < \theta < \theta_1$.
- α_4 versus α_5 in the range $\theta_1 < \theta < \theta_{\max}$.

Between above two α_k 's, the following lemmas are satisfied.

Lemma 3 There exists θ_{36} such that $\alpha_6(\theta) < \alpha_3(\theta)$ in the range $\theta_{36} < \theta < \theta_{36} + \pi$, while $\alpha_3(\theta) < \alpha_6(\theta)$ in the range $\theta_{36} - \pi < \theta < \theta_{36}$. This θ_{36} is given as follows:

$$\theta_{36} = \arctan2(B_{36}, A_{36}) \tag{36}$$

where

$$A_{36} = y (\tan(\phi_1 + \xi_1) + \tan(\phi_2 - \xi_2)) - (x_1 + x_2) \tag{37}$$

$$B_{36} = x_2 \tan(\phi_1 + \xi_1) - x_1 \tan(\phi_2 - \xi_2) \tag{38}$$

Lemma 4 There exists θ_{45} such that $\alpha_4(\theta) < \alpha_5(\theta)$ in the range $\theta_{45} < \theta < \theta_{45} + \pi$, while $\alpha_5(\theta) < \alpha_4(\theta)$ in the range $\theta_{45} - \pi < \theta < \theta_{45}$. This θ_{45} is given as follows:

$$\theta_{45} = \arctan2(B_{45}, A_{45}) \tag{39}$$

where

$$A_{45} = y (\tan(\phi_1 - \xi_1) + \tan(\phi_2 + \xi_2)) - (x_1 + x_2) \tag{40}$$

$$B_{45} = x_2 \tan(\phi_1 - \xi_1) - x_1 \tan(\phi_2 + \xi_2) \tag{41}$$

Lemma 5 There exists θ_{34} such that $\alpha_3(\theta) < \alpha_4(\theta)$ in the range $\theta_{34} < \theta < \theta_{34} + \pi$, while $\alpha_4(\theta) < \alpha_3(\theta)$ in the range $\theta_{34} - \pi < \theta < \theta_{34}$. This θ_{34} is given as follows:

$$\theta_{34} = \arctan2(B_{34}, A_{34}) \tag{42}$$

where

$$A_{34} = (x_1 + x_2) - y (\tan(\phi_1 + \xi_1) + \tan(\phi_2 + \xi_2)) \tag{43}$$

$$B_{34} = x_1 \tan(\phi_2 + \xi_2) - x_2 \tan(\phi_1 + \xi_1) \tag{44}$$

The proof for the Lemma 5 is shown below:

Proof From (30) and (31), we obtain

$$\begin{aligned} \alpha_4 - \alpha_3 &= 2 \{ (x_1 + x_2) - y (\tan(\phi_1 + \xi_1) + \tan(\phi_2 + \xi_2)) \} \sin \theta \\ &\quad - 2 \{ x_1 \tan(\phi_2 + \xi_2) - x_2 \tan(\phi_1 + \xi_1) \} \cos \theta \\ &= 2(A_{34} \sin \theta - B_{34} \cos \theta) \\ &= 2\sqrt{A_{34}^2 + B_{34}^2} \sin(\theta - \theta_{34}) \end{aligned} \tag{45}$$

Then, it is trivial from the above equation. \square

The Lemmas 3 and 4 can be proven in the same way.

D Analysis of minimal solution

Finally, the calculations of the last Step 4 in Sect. 3.1 are described. The five candidates of the local minimum point are obtained: θ_{36} , θ_{34} , θ_{45} , and the boundaries of the analyzed range θ_{\min} , θ_{\max} . How are these candidates physically explained, and what magnitude relations are satisfied among them?

At first, the next lemma is obtained regarding to θ_{34} .

Lemma 6 *When the gravitational direction is given as θ_{34} , the CoM of the object and \mathbf{p}_{uu} vertically align on the gravity line in the task coordinate frame. Then, \mathbf{p}_{uu} is positioned above the CoM of the object.*

Proof Let the relative angle to the point \mathbf{p}_{uu} from the negative direction of the y axis to θ_{uu} . Then, the equation $\theta_{uu} = \theta_{34} \pm \pi$ should be derived since the origin of the object coordinate frame is set to the CoM of the object.

$\mathbf{p}_{uu}(X_{uu}, Y_{uu})$ is located on the line ℓ_1^u that passes through the point (x_1, y) and whose slope is given as $\tan(\frac{\pi}{2} - \phi_1 - \xi_1) = \cot(\phi_1 + \xi_1)$. Thus, X_{uu} and Y_{uu} satisfy the next equation.

$$Y_{uu} - y = \cot(\phi_1 + \xi_1)(X_{uu} - x_1) \tag{46}$$

\mathbf{p}_{uu} is also located on the line ℓ_2^u that passes through the point $(-x_2, y)$ and whose slope is given as $\tan(\phi_2 + \xi_2 - \frac{\pi}{2}) = -\cot(\phi_2 + \xi_2)$. So, in the same way,

$$Y_{uu} - y = -\cot(\phi_2 + \xi_2)(X_{uu} + x_2) \tag{47}$$

From the above two equation, X and Y are given as follows:

$$X_{uu} = \frac{x_1 \tan(\phi_2 + \xi_2) - x_2 \tan(\phi_1 + \xi_1)}{\tan(\phi_1 + \xi_1) + \tan(\phi_2 + \xi_2)} \tag{48}$$

$$Y_{uu} = \frac{y(\tan(\phi_1 + \xi_1) + \tan(\phi_2 + \xi_2)) - (x_1 + x_2)}{\tan(\phi_1 + \xi_1) + \tan(\phi_2 + \xi_2)} \tag{49}$$

Now, let $T_{uu} = \tan(\phi_1 + \xi_1) + \tan(\phi_2 + \xi_2)$, then $T_{uu} < 0$ from (1). Thus, θ_{uu} is given by

$$\begin{aligned} \theta_{uu} &= \arctan2(X_{uu}, -Y_{uu}) = \arctan2\left(\frac{B_{34}}{T_{uu}}, -\left(\frac{-A_{34}}{T_{uu}}\right)\right) \\ &= \arctan2(-B_{34}, -A_{34}) = \theta_{34} \pm \pi \end{aligned} \tag{50}$$

Now, lemma is proven. □

In the similar way, the following lemmas holds.

Lemma 7 *When the gravitational direction is given as θ_{36} , \mathbf{p}_{ul} and the CoM of the object vertically align on the gravity line in the task coordinate frame. If the slope of ℓ_2^ℓ is negative as well as greater than that of ℓ_1^u , \mathbf{p}_{ul} is positioned above the CoM. Otherwise, \mathbf{p}_{ul} is positioned below the CoM.*

Lemma 8 *When the gravitational direction is given as θ_{45} , \mathbf{p}_{lu} and the CoM of the object vertically align on the gravity line in the task coordinate frame. If the slope of ℓ_1^ℓ is positive as well as less than that of ℓ_2^u , \mathbf{p}_{lu} is positioned above the CoM. Otherwise, \mathbf{p}_{lu} is positioned below the CoM.*

Because of the symmetry, only the proof of Lemma 7 is shown.

Proof Let the relative angle to the point \mathbf{p}_{ul} from the negative direction of the y axis to θ_{ul} . And, let $T_{ul} = \tan(\phi_1 + \xi_1) + \tan(\phi_2 - \xi_2) (\neq 0)$. Note that, if the slope of ℓ_2^ℓ is negative and greater than that of ℓ_1^u , then $T_{ul} > 0$. Otherwise $T_{ul} < 0$. Because $\mathbf{p}_{ul}(X_{ul}, Y_{ul})$ is located on ℓ_1^u as well as ℓ_2^ℓ , the next two equations hold.

$$Y_{ul} - y = \cot(\phi_1 + \xi_1)(X_{ul} - x_1) \tag{51}$$

$$Y_{ul} - y = -\cot(\phi_2 - \xi_2)(X_{ul} + x_2) \tag{52}$$

These equations are solved as

$$X_{ul} = \frac{x_1 \tan(\phi_2 - \xi_2) - x_2 \tan(\phi_1 + \xi_1)}{\tan(\phi_1 + \xi_1) + \tan(\phi_2 - \xi_2)} \tag{53}$$

$$Y_{ul} = \frac{y(\tan(\phi_1 + \xi_1) + \tan(\phi_2 - \xi_2)) - (x_1 + x_2)}{\tan(\phi_1 + \xi_1) + \tan(\phi_2 - \xi_2)} \tag{54}$$

Then, θ_{ul} is given by

$$\begin{aligned} \theta_{ul} &= \arctan2(X_{ul}, -Y_{ul}) \\ &= \arctan2\left(-\frac{B_{36}}{T_{ul}}, -\frac{A_{36}}{T_{ul}}\right) \end{aligned} \tag{55}$$

If $T_{ul} > 0$, $\theta_{ul} = \arctan2(-B_{36}, -A_{36}) = \theta_{36} \pm \pi$, implying that \mathbf{p}_{ul} is located in the opposite direction of the gravity. On the contrary, If $T_{ul} < 0$, $\theta_{ul} = \theta_{36}$, and so \mathbf{p}_{ul} is located in the same direction of the gravity. □

Note that, when $T_{ul} = 0$, ℓ_1^u , and ℓ_2^ℓ are parallel. Thus, \mathbf{p}_{ul} does not exist. In this case, the gravitational direction θ_{36} become parallel to ℓ_1^u as well as ℓ_2^ℓ .

From the above lemmas, the following magnitude relation can be obtained in a graphical manner,

$$-(\theta_1 + \pi) < \theta_{36} < -\theta_1 < \theta_{34} < \theta_2 < \theta_{45} < \theta_2 + \pi \tag{56}$$

Using the above all facts, $\alpha_{\min}(\theta)$, which is defined in the step 3 of Sect. 3.1, is given as follows:

$$\alpha_{\min}(\theta) = \begin{cases} \alpha_6(\theta) & (\theta \leq \theta_{36}) \\ \alpha_3(\theta) & (\theta_{36} \leq \theta \leq \theta_{34}) \\ \alpha_4(\theta) & (\theta_{34} \leq \theta \leq \theta_{45}) \\ \alpha_5(\theta) & (\theta_{45} \leq \theta) \end{cases} \tag{57}$$

Furthermore, the magnitude relation between θ_{36} and θ_{\min} as well as θ_{45} and θ_{\max} is classified into four cases according to the spatial relation among the friction cones and the CoM of the object. This classification is illustrated in Fig. 6. Finally, the theorem in Sect. 3.2 is obtained as for the object orientation minimizing the gripping power.

References

Al-Gallaf EA (2006) Multi-fingered robot hand optimal task force distribution neural inverse kinematics approach. Robot Auton Syst 54:34–51

- Arimoto S, Tahara K, Yamaguchi M, Nguyen PTA, Han MY (2001) Principles of superposition for controlling pinch motions by means of robot fingers with soft tips. *Robotica* 19(01):21–28
- Berenson D, Srinivasa S (2008) Grasp synthesis in cluttered environments for dexterous hands. In: *Robotics Science and Systems (RSS) workshop on robot manipulation: intelligence in human environments*
- Bicchi A (1995) On the closure properties of robotic grasping. *Int J Robot Res* 14(4):319–334
- Borst C, Fischer M, Hirzinger G (1999) A fast and robust grasp planner for arbitrary 3D objects. In: *1999 IEEE international conference on robotics and automation, 1999. Proceedings, vol 3*
- Cheng F-T, Orin DE (1990) Efficient algorithm for optimal force distribution – the compact-dual lp method. *IEEE Trans. on Robotics and Automation* 6(2):178–187
- Ciocarlie M, Lackner C, Allen P (2007) Soft finger model with adaptive contact geometry for grasping and manipulation tasks. In: *Euro-Haptics conference, 2007 and symposium on haptic interfaces for virtual environment and teleoperator systems. World Haptics 2007, Second Joint, pp 219–224*
- Cole KJ, Abbs JH (1987) Kinematic and electromyographic responses to perturbation of a rapid grasp. *J Neurophysiol* 57(5):1498–1510
- Ding D, Liu Y-H, Wang MY, Wang S (2001) Automatic selection of fixturing surfaces and fixturing points for polyhedral workpieces. *IEEE Trans Robot Autom* 17(6):833–841
- Dollar AM, Howe RD (2005) Towards grasping in unstructured environments: Grasper compliance and configuration optimization. *Adv Robot* 19(5):523–544
- Dubey VN, Crowder RM, Chappell PH (1999) Optimal object grasp using tactile sensors and fuzzy logic. *Robotica* 17:685–693
- Frey SH, Vinton D, Norlund R, Grafton ST (2005) Cortical topography of human anterior intraparietal cortex active during visually guided grasping. *Cogn Brain Res* 23(2-3):397–405
- Huebner K, Ruthotto S, Kragic D (2008) Minimum volume bounding box decomposition for shape approximation in robot grasping. In: *IEEE International conference on robotics and automation, 2008. ICRA 2008, pp 1628–1633*
- Iberall T, MacKenzie CL (1990) Opposition space and human prehension. In: *Venkataraman ST, Iberall T (eds) Dexterous robot hands. Springer, New York, p 32*
- Ito S, Mizukoshi Y, Ishihara K, Sasaki M (2006) Optimal direction of grasped object minimizing contact forces. In: *Proceedings of the 2006 IEEE/RSJ international conference on intelligent robots and systems, pp 1588–1593*
- Ito S, Mizukoshi Y, Sasaki M (2007) Numerical analysis for optimal posture of circular object grasped with frictions. In: *Proceedings of the 2007 IEEE/RSJ international conference on intelligent robots and systems*
- Liu Y-H (1999) Qualitative test and force optimization of 3-d frictional form-closure grasps using linear programming. *IEEE Trans Robot Autom* 15(1):163–173
- Lopez-Damian E, Sidobre D, Alami R (2005) Grasp planning for non-convex objects. In: *International symposium on robotics, vol 36. Citeseer, p 167*
- Mangialardi L, Mantriota G, Trentadue A (1996) A three-dimensional criterion for the determination of optimal grip points. *Robot Comput-Integr Manuf* 12(2):157–167
- Markenscoff X, Papadimitriou CH (1989) Optimal grip of a polygon. *Int J Robot Res* 8(2):17–29
- Miller AT, Allen PK (2000) GraspIt!: a versatile simulator for grasping analysis. In: *Proceedings of the ASME dynamic systems and control division*
- Miller AT, Knoop S, Christensen HI, Allen PK (2003) Automatic grasp planning using shape primitives. In: *Proceedings of IEEE international conference on robotics and automation (ICRA'03), vol 2*
- Mirtich B, Canny J (1994) Easily computable optimum grasps in 2-d and 3-d. In: *Proceedings of IEEE international conference on robotics and automation (ICRA'94), pp 739–747*
- Nakamura Y, Kurushima S (1997) Computation of marginal external force space of power grasp using polyhedral convex set theory. *J Robot Soc Jpn* 15(5):728–735
- Nguyen VD (1988) Constructing force closure grasp. *Int J Robot Res* 7(3):3–16
- Omata T (1993) Finger position computation for 3-dimensional equilibrium grasps. In: *Proceedings of IEEE international conference on robotics and automation (ICRA'93), vol 2, pp 216–222*
- Oztop E, Arbib MA (2002) Schema design and implementation of the grasp-related mirror neuron system. *Biol Cybernet* 87(2):116–140
- Roa MA, Suárez R (2009) Finding locally optimum force-closure grasps. *Robot Comput Integr Manuf* 25(3):536–544
- Shim JK, Latash ML, Zatsiorsky VM (2003) Prehension synergies: trial-to-trial variability and hierarchical organization of stable performance. *Exp Brain Res* 152(2):173–184
- Shimoga KB (1996) Robot grasp synthesis algorithms: a survey. *Int J Robot Res* 15(3):230–266
- Watanabe T, Yoshikawa T (2003) Optimization of grasping by using a required external force set. In: *Proceedings of IEEE international conference on robotics and automation (ICRA2003), pp 1127–1132*
- Xia Y, Wang J, Fok L-M (2004) Grasping-force optimization for multi-fingered robotic hands using a recurrent neural network. *IEEE Trans Robot Autom* 20(3):549–554
- Yong Y, Takeuchi K, Yoshikawa T (1998) Optimization of robot hand power grasps. In: *Proceedings of IEEE international conference on robotics and automation (ICRA'98), vol 4, pp 3341–3347*
- Zatsiorsky VM, Latash ML (2008) Multifinger prehension: an overview. *J Motor Behav* 40(5):446–476
- Zhang X-Y, Nakamura Y, Goda K, Yoshimoto K (1994) Robustness of power grasp. In: *Proceedings of IEEE international conference on robotics and automation (ICRA'94), vol 4, pp 2828–2835*